Pis'ma v ZhETF, vol. 96, iss. 6, pp. 436 – 443

Nature of the quantum critical point as disclosed by extraordinary behavior of magnetotransport and the Lorentz number in the heavy-fermion metal $YbRh_2Si_2$

V. R. Shaginyan[+*1)], *A. Z. Msezane*[*], *K. G. Popov*[×], *J. W. Clark*[°], *M. V. Zverev*[∇△], *V. A. Khodel*[∇°]

[+]*Petersburg Nuclear Physics Institute, 188300 Gatchina, Russia*

[*]*Clark Atlanta University, GA 30314 Atlanta, USA*

[×]*Komi Science Center UD of the RAS, 167982 Syktyvkar, Russia*

[°]*McDonnell Center for the Space Sciences & Department of Physics, Washington University, St. Louis, MO 63130, USA*

[∇]*Russian Research Centre "Kurchatov Institute", 123182 Moscow, Russia*

[△]*Moscow Institute of Physics and Technology, 123098 Moscow, Russia*

Submitted 20 July 2012
Resubmitted 6 August 2012

Physicists are engaged in vigorous debate on the nature of the quantum critical points (QCP) governing the low-temperature properties of heavy-fermion (HF) metals. Recent experimental observations of the much-studied compound $YbRh_2Si_2$ in the regime of vanishing temperature incisively probe the nature of its magnetic-field-tuned QCP. The jumps revealed both in the residual resistivity ρ_0 and the Hall resistivity R_H, along with violation of the Wiedemann–Franz law, provide vital clues to the origin of such non-Fermi-liquid behavior. The empirical facts point unambiguously to association of the observed QCP with a fermion-condensation phase transition. Based on this insight, the resistivities ρ_0 and R_H are predicted to show jumps at the crossing of the QCP produced by application of a magnetic field, with attendant violation of the Wiedemann–Franz law. It is further demonstrated that experimentally identifiable multiple energy scales are related to the scaling behavior of the effective mass of the quasiparticles responsible for the low-temperature properties of such HF metals.

A quantum critical point (QCP) dictates the non-Fermi liquid (NFL) low-temperature properties of strongly correlated Fermi systems, notably heavy fermion (HF) metals, high-temperature superconductors, and quasi-two-dimensional ^{3}He. Their NFL behavior is so radical that the traditional Landau quasiparticle paradigm is at a loss to describe it. The underlying nature of the QCP has continued to defy theoretical understanding. Attempts have been made using concepts such as the Kondo lattice and involving quantum and thermal fluctuations at the QCP [1–5]. Alas, when designed to describe one property deemed central, these approaches fail to explain others, even the simplest ones such as the Kadowaki–Woods relation [6, 7]. This relation, which emerges naturally when quasiparticles of effective mass M^* play the main role, can hardly be explained within the framework of a theory that presupposes the absence of quasiparticles at the QCP (for recent reviews see [7–9]). Arguments that quasiparticles in strongly correlated Fermi liquids "get heavy and die" at the QCP commonly employ the assumption that the quasiparticle weight factor Z vanishes at the point of an associated second-order phase transition [10, 11]. However, this scenario is problematic [12, 13]. Numerous experimental facts have been discussed in terms of such a framework, but how it can explain the physics of HF metals quantitatively is left as an open question [7]. A theory of fermion condensation (FC) that preserves quasiparticles while being intimately related to the unlimited growth of M^* has been proposed and developed [7–9, 14, 15]. Extensive studies have shown that this theory delivers an adequate theoretical explanation of the great majority of experimental results in different HF metals. In contrast to the Landau paradigm based on the assumption that M^* is a constant, within FC theory M^* depends strongly on both temperature T and imposed magnetic field B. Accordingly, an extended quasiparticle paradigm is introduced. The essential point is that – as before – well-defined quasiparticles determine the thermodynamic and transport properties of strongly correlated Fermi systems, while the dependence of the

[1)] e-mail: vrshag@thd.pnpi.spb.ru

effective mass M^* on T and B gives rise to the observed NFL behavior [7–9]. The most fruitful strategy for exploring and revealing the nature of the QCP is to focus on those properties that exhibit the most spectacular departures from Landau–Fermi Liquid (LFL) behavior in the zero-temperature limit. In particular, incisive experimental measurements recently performed on the heavy-fermion metal $YbRh_2Si_2$ have probed the nature of its magnetic-field-tuned QCP. It is found that at vanishingly low temperatures the residual resistivity ρ_0 experiences a jump across the magnetic QCP, with a crossover regime proportional to T [16–19]. Jumps of the magnetoresistivity, the Hall coefficient, and the Lorenz number at zero temperature are in conflict with the common behavior of Kondo systems, for which the width of the change remains finite at zero temperature [19, 20]. Under the same experimental conditions in $YbRh_2Si_2$, the Hall coefficient R_H is also found to experience a jump [17], while the data collected on heat and charge transport at the QCP can be interpreted as indicating a violation of the Wiedemann–Franz law [19]. The Wiedemann–Franz law defines the value of the Lorentz number $L = \kappa/T\sigma$ at $T \to 0$, i.e., $L = L_0$ with $L_0 = (\pi k_B)^2/3e^2$, where κ, σ, k_B, and e are respectively the thermal conductivity, the electrical conductivity, Boltzmann's constant, and the charge of the electron.

In this Letter we study magnetotransport and violation of the Wiedemann–Franz law in $YbRh_2Si_2$ across a QCP tuned by application of a magnetic field. Close similarity between the behavior of the Hall coefficient R_H and magnetoresistivity ρ at QCP indicates that all manifestations of magnetotransport stem from the same underlying physics. We show that the violation of the Wiedemann–Franz law together with the jumps of the Hall coefficient and magnetoresistivity in the zero-temperature limit provide unambiguous evidence for interpreting the QCP in terms of a fermion condensation quantum phase transition (FCQPT) forming a flat band in $YbRh_2Si_2$.

We begin with an analysis of the scaling behavior of the effective mass M^* and $T-B$ phase diagram of a homogeneous HF liquid, thereby avoiding complications associated with the crystalline anisotropy of solids [7]. Near the FCQPT, the temperature and magnetic field dependence of the effective mass $M^*(T,B)$ is governed by the Landau equation [21]

$$\frac{1}{M^*_\sigma(T,B)} = \frac{1}{m} + \sum_{\sigma_1}\int \frac{\mathbf{p}_F\mathbf{p}}{p_F^3} F_{\sigma,\sigma_1}(\mathbf{p}_F,\mathbf{p}) \times \times \frac{\partial n_{\sigma_1}(\mathbf{p},T,B)}{\partial p}\frac{d\mathbf{p}}{(2\pi)^3}, \quad (1)$$

where $F_{\sigma,\sigma_1}(\mathbf{p}_F,\mathbf{p})$ is the Landau interaction, p_F is the Fermi momentum, and σ is the spin label. To simplify matters, we ignore the spin dependence of the effective mass, noting that $M^*(T,B)$ is nearly independent of spin in weak fields. The quasiparticle distribution function n can be expressed as

$$n_\sigma(\mathbf{p},T) = \left(1 + \exp\left\{\frac{[\varepsilon(\mathbf{p},T) - \mu_\sigma]}{T}\right\}\right)^{-1}, \quad (2)$$

where $\varepsilon(\mathbf{p},T)$ is the single-particle (sp) spectrum. In the case being considered, the sp spectrum depends on spin only weakly. However, the chemical potential μ_σ depends non-trivially on spin due to the Zeeman splitting, $\mu_\pm = \mu \pm B\mu_B$, where "$\pm$" corresponds to states with the spin "up" or "down." Numerical and analytical solutions of this equation show that the dependence $M^*(T,B)$ of the effective mass gives rise to three different regimes with increasing temperature. In the theory of fermion condensation, if the system is located near the FCQPT on its ordered side, then the fermion condensate (FC) represents a group of sp states with dispersion given by [22]

$$\varepsilon(\mathbf{p},n) - \mu = T\ln\frac{1-n(\mathbf{p})}{n(\mathbf{p})}, \quad (3)$$

where μ is the chemical potential and $n(\mathbf{p})$ is the quasiparticle occupation number, which loses its temperature dependence at sufficiently low T. On the ordered side the sp spectrum of the HF liquid contains a flat portion embracing the Fermi surface; on the other hand, on the disordered side, at fixed, finite B and low temperatures we have a LFL regime with $M^*(T) \simeq M^* + aT^2$, where a is a positive constant [7]. Thus the effective mass grows as a function of T, reaching its maximum M^*_M at some temperature T_M and subsequently diminishing according to [23]

$$M^*(T) \propto T^{-2/3}. \quad (4)$$

Moreover, the closer the control parameter B is to its critical value $B_{c0} = 0$, the higher the growth rate. In this case, the peak value of M^*_M also grows, but the temperature T_M at which M^* reaches its peak value decreases, so that $M^*_M(T_M, B \to B_{c0}) \to \infty$. At $T > T_M$, the last traces of LFL disappear. When the system is in the vicinity of the FCQPT, the approximate interpolative solution of Eq. (1) reads [7]

$$\frac{M^*}{M^*_M} = M^*_N(T_N) \approx c_0\frac{1 + c_1T_N^2}{1 + c_2T_N^{8/3}}. \quad (5)$$

Here, $T_N = T/T_M$ is the normalized temperature, with $c_0 = (1+c_2)/(1+c_1)$ in terms of fitting parameters c_1

and c_2. Since the magnetic field enters Eq. (2) in the form $\mu_B B/T$, we conclude that

$$T/T_M \propto \frac{T}{\mu_B B}, \tag{6}$$

where μ_B is the Bohr magneton. It follows from Eq. (6) that

$$T_M \simeq a_1 \mu_B B. \tag{7}$$

Equation (5) reveals the scaling behavior of the normalized effective mass $M^*_N(T_N)$: values of the effective mass $M^*(T,B)$ at different magnetic fields B merge into a single mass value M^*_N in terms of the normalized variable $T_N = T/T_M$ [7]. The inset in Fig. 1 demonstrates

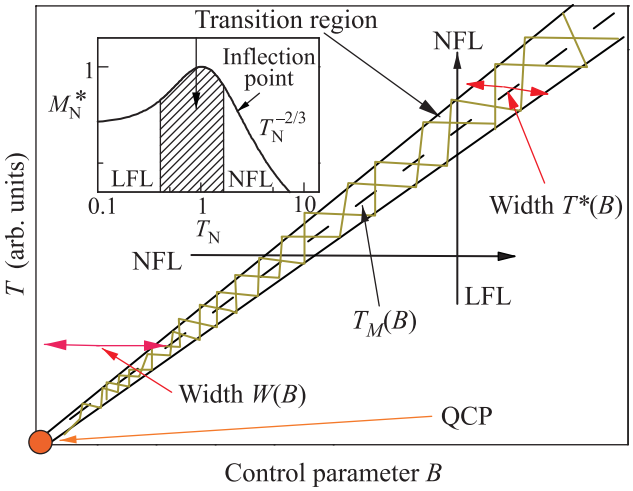

Fig. 1. (Color online) Schematic $T-B$ phase diagram of HF liquid with magnetic field as the control parameter. The vertical and horizontal arrows show LFL–NFL and NFL–LFL transitions at fixed B and T, respectively. At $B = 0$ the system is in its NFL state having a flat band and demonstrates NFL behavior down to $T \to 0$. The hatched area separates the NFL phase and the weakly polarized LFL phase and represents the transition area. The dashed line in the hatched area represents the function $T_M(B)$ given by Eq. (7). The functions $W(B) \propto T$ and $T^*(B) \propto T$ shown by two-headed arrows define the width of the NFL state and the transition area, respectively. The QCP located at the origin and indicated by an arrow denotes the critical point at which the effective mass M^* diverges and both $W(B)$ and $T^*(B)$ tend to zero. The inset shows a schematic plot of the normalized effective mass versus the normalized temperature. The transition regime, where M^*_N reaches its maximum value at $T_N = T/T_M = 1$, is shown as the hatched area in both the main panel and the inset. Arrows indicate the transition region and the inflection point T_{inf} in the M^*_N plot

the scaling behavior of the normalized effective mass M^*_N versus the normalized temperature T_N. The LFL phase prevails at $T \ll T_M$, followed by the $T^{-2/3}$ regime at $T \gtrsim T_M$. The latter phase is designated as NFL due to the strong dependence of the effective mass on temperature. The temperature region $T \simeq T_M$ encompasses the transition between the LFL regime with almost constant effective mass and the NFL behavior described by Eq. (4). Thus $T \sim T_M$ identifies the transition region featuring a crossover between LFL and NFL regimes. The inflection point T_{inf} of M^*_N versus T_N is depicted by an arrow in the inset of Fig. 1.

The transition (crossover) temperature $T_M(B)$ is not actually the temperature of a phase transition. Its specification is necessarily ambiguous, depending as it does on the criteria invoked for determination of the crossover point. As usual, the temperature $T^*(B)$ is extracted from the field dependence of charge transport, for example from the resistivity $\rho(T)$ given by

$$\rho(T) = \rho_0 + AT^{\alpha_R}, \tag{8}$$

where ρ_0 is the residual resistivity and A is a T-independent coefficient. The term ρ_0 is ordinarily attributed to impurity scattering. The LFL state is characterized by the T^{α_R} dependence of the resistivity with index $\alpha_R = 2$. The crossover (through the transition regime shown as the hatched area in both Fig. 1 and its inset) takes place at temperatures where the resistance starts to deviate from LFL behavior, with the exponent α_R shifting from 2 into the range $1 < \alpha_R < 2$. The schematic phase diagram of a HF metal is depicted in Fig. 1, with the magnetic field B serving as the control parameter. At $B = 0$, the HF liquid acquires a flat band corresponding to a strongly degenerate state. The NFL regime reigns at elevated temperatures and fixed magnetic field. With increasing B, the system is driven from the NFL region to the LFL domain. As shown in Fig. 1, the system moves from the NFL regime to the LFL regime along a horizontal arrow, and from the LFL to NFL along a vertical arrow. The magnetic-field-tuned QCP is indicated by an arrow and located at the origin of the phase diagram, since application of a magnetic field destroys the flat band and shifts the system into the LFL state [7, 8, 9]. The hatched area denoting the transition region separates the NFL state from the weakly polarized LFL state and contains the dashed line tracing $T_M(B)$. Referring to Eq. (7), this line is defined by the function $T = a_1 \mu_B B$, and the width $W(B)$ of the NFL state is seen to be proportional T. In the same way, it can be shown that the width $T^*(B)$ of the transition region is also proportional to T.

In this letter we focus on the HF metal $YbRh_2Si_2$, whose empirical $T-B$ phase diagram is reproduced in panels a and b of Fig. 2. Panel a is similar to the

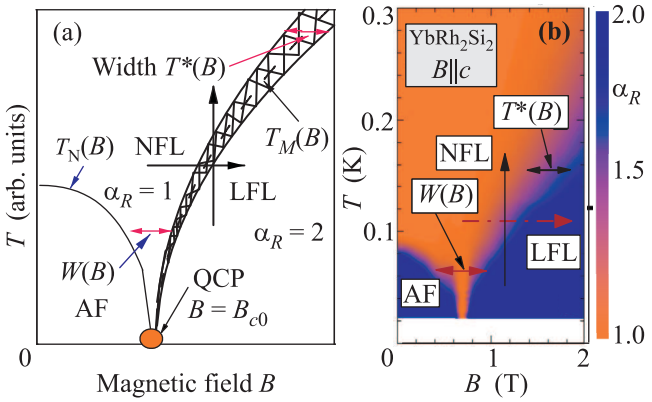

Fig. 2. (Color online) Panel a represents a schematic phase diagram of the HF metal $YbRh_2Si_2$, with $T_N(B)$ denoting the Nèel temperature as a function of magnetic field B. The QCP, identified by an arrow, is now shifted to $B = B_{c0}$. At $B < B_{c0}$ the system is in its antiferromagnetic (AF) state, denoted by AF. As in Fig. 1, the vertical and horizontal arrows show the transitions between the LFL and NFL states, the functions $W(B) \propto T$ and $T^*(B) \propto T$ indicated with bi-directional arrows define the width of the NFL state and of the transition region, respectively, and the dashed line in the hatched area represents the function $T_M(B)$ given by Eq. (7). The exponent α_R determines the temperature-dependent part of the resistivity (cf. Eq. (8)), with α_R taking values 2 and 1, respectively, in LFL and NFL states. In the transition regime the exponent evolves between LFL and NFL values. Panel b shows the experimental $T-B$ phase diagram [27, 19]. The evolution of α_R is depicted by color (coded in the vertical stripe on the right-hand side of the panel). The NFL behavior reaches to the lowest temperatures right at the QCP tuned by the magnetic field. The transition regime between the NFL state and the field-induced LFL state broadens with rising magnetic fields $B > B_{c0}$ and $T \sim T^*(B)$. As in panel a, transitions from LFL to NFL state and from NFL to LFL state are indicated by the corresponding arrows, as are $W(B) \propto T$ and $T^*(B) \propto T$

main panel of Fig. 1, but with the distinction that this HF compound possesses a finite critical magnetic field $B_{c0} \neq 0$ that shifts the QCP from the origin. To avert realization of a strongly degenerate ground state induced by the flat band, the FC must be completely eliminated at $T \to 0$. In a natural scenario, this occurs by means of an antiferromagnetic (AF) phase transition with an ordering temperature $T_N = 70\,\mathrm{mK}$, while application of a magnetic field $B = B_{c0}$ destroys the AF state at $T = 0$ [24]. In other words, the field B_{c0} places the HF metal at the magnetic-field-tuned QCP and nullifies the Nèel temperature $T_N(B_{c0}) = 0$ of the corresponding AF phase transition [7, 25]. Imposition of a magnetic field $B > B_{c0}$ drives the system to the LFL state. Thus, in the case of $YbRh_2Si_2$, the QCP is shifted from the origin to $B = B_{c0}$. In FC theory, the quantity B_{c0} is a parameter determined by the properties of the specific heavy-fermion metal. In some cases, notably the HF metal $CeRu_2Si_2$, B_{c0} does vanish [26], whereas in $YbRh_2Si_2$, $B_{c0} \simeq 0.06$ T, $B \perp c$ [24].

Panel b of Fig. 2 portrays the experimental $T-B$ phase diagram in a manner showing the evolution of the exponent $\alpha_R(T, B)$ [27, 19]. At the critical field $B_{c0} \simeq 0.66$ T ($\mathbf{B} \| \mathbf{c}$), the NFL behavior extends down to the lowest temperatures, while $YbRh_2Si_2$ transits from the NFL to LFL behavior under increase of the applied magnetic field. Vertical and the horizontal arrows indicate, respectively, the transition from the LFL to the NFL state and its reversal. The functions $W(B) \propto T$ and $T^*(B) \propto T$ associated with bi-directed arrows define the width of the NFL state and transition region, respectively. It noteworthy that the schematic phase diagram displayed in panel a of Fig. 2 is in close qualitative agreement with its experimental counterpart in panel b.

To calculate the low-temperature dependence of ρ on the imposed magnetic field B in the normal state of $YbRh_2Si_2$, we employ a model of a HF liquid possessing a flat band with dispersion given by Eq. (3). Since the resistivity at $T \to 0$ is our primary concern, we concentrate on a special contribution to the residual resistivity ρ_0 which we call the critical residual resistivity ρ_0^c. Analysis begins with the case $B = 0$, for which the resistivity of the HF liquid at low temperatures is a linear function of T [7, 28]. This observation is in accord with experimental facts derived from measurements on $YbRh_2Si_2$ indicating the presence of a flat band in $YbRh_2Si_2$ [24, 7, 28, 29]. In that case, the effective mass $M^*(T)$ of the FC quasiparticles takes the form

$$M^*(T) \sim \frac{\eta p_F^2}{4T}, \tag{9}$$

where $\eta = \delta p / p_F$ is determined by the characteristic size δp of the momentum interval L occupied by the FC [30]. With the result (9) the width γ of FC quasiparticles is calculated in closed form, $\gamma \sim \gamma_0 + \eta T$, where γ_0 is a constant [30]. This result leads to the lifetime τ_q of quasiparticles

$$\hbar/\tau_q \simeq a_1 + a_2 T, \tag{10}$$

where $\hbar$ is Planck's constant, a_1 and a_2 are parameters. Equation (10) is in excellent agreement with experimental observations [31]. In general the electronic liquid in HF metals is represented by several bands occupied by quasiparticles that simultaneously intersect the Fermi surface, and FC quasiparticles never cover

the entire Fermi surface. Thus there exist LFL quasiparticles with the effective mass M_L^* independent of T and FC quasiparticles with M^* given by Eq. (9) at the Fermi surface, and all of them possess the same width γ. Upon appealing to the standard equation

$$\sigma \sim \frac{Ne^2}{\gamma M^*} \tag{11}$$

for the conductivity σ (see e.g. [21]) and taking into account the formulas specifying M^* and γ, we find that $\sigma \sim Ne^2/(p_{\rm F}\eta)^2$, where N is the number density of electrons. With this result, we arrive at a critical residual resistivity ρ_0^c that is independent of T:

$$\rho_0^c \sim \frac{\eta^2}{p_{\rm F}e^2}. \tag{12}$$

Careful derivation and examination of Eqs. (11) and (12) is provided in [30]. The term "residual resistivity" is ordinarily attributed to impurity scattering. In the present case, Eq. (12) shows that ρ_0^c is determined by the presence of a flat band and has no relation to the scattering quasiparticles by impurities.

We next demonstrate that the application of a magnetic field to the HF liquid generates the observed step-like drop in the residual resistivity ρ_0. Indeed, Fig. 1 informs us that at fixed temperature, application of the field B drives the system from the NFL state to the LFL state, the flat portion of $\varepsilon(\mathbf{p})$ determined by Eq. (3) being destroyed at $T < T_M$ [7]. Thereupon the factor η vanishes, nullifying ρ_0^c and strongly reducing ρ_0. Since both $W(B)$ and $T^*(B)$ widths are proportional T, imposition of the magnetic field causes a step-like drop in the residual resistivity ρ_0. Consequently two values of the residual resistivity must be introduced, namely $\rho_0^{\rm NFL}$ corresponding to the NFL state and $\rho_0^{\rm LFL}$ corresponding to the LFL state induced upon application of the magnetic field B. It follows from these considerations that $\rho_0^{\rm NFL} > \rho_0^{\rm LFL}$. This conclusion agrees with the experimental findings [16, 17, 19].

Fig. 2 shows the $T-B$ phase diagram of $YbRh_2Si_2$, which maps faithfully onto the schematic phase diagram depicted in Fig. 1, except for the appearance of an AF phase at low temperatures. As seen from Fig. 2, at $T > T_{\rm N}$ and $B = 0$ the system in its NFL state, while the LFL phase prevails at low temperature for magnetic fields beyond the critical value B_{c0}. The respective residual resistivities are measured at $\rho_0^{\rm NFL} \simeq \simeq 0.55\,\mu\Omega\cdot$cm (NFL) and $\simeq 0.5\,\mu\Omega\cdot$cm (LFL) [16]. As T is lowered through $T_{\rm N}$ at $B = 0$ the system enters the AF state via a second-order phase transition. Accordingly, we expect that the residual resistivity does not change, remaining the same as that of the NFL state, $\rho_0^{\rm NFL}$. On the other hand, under imposition of an increasing B-field, the system moves from the NFL state to the LFL state with the above value of $\rho_0^{\rm LFL}$. At this point it should be acknowledged that application of a weak magnetic field is known to produce a positive classical contribution $\propto B^2$ to ρ_0 arising from orbital motion of carriers induced by the Lorentz force. When considering spin-orbit coupling in disordered electron systems where electron motion is diffusive, the magnetoresistivity may have both positive (weak localization) and negative (weak anti-localization) signs [32]. However, as studied experimentally, $YbRh_2Si_2$ is one of the purest heavy-fermion metals. Hence the applicable regime of electron motion is ballistic rather than diffusive, both weak and anti-weak localization scenarios are irrelevant, and one expects the B-dependent correction to ρ_0 to be positive. We therefore conclude that the positive difference $\rho_0^c = \rho_0^{\rm NFL} - \rho_0^{\rm LFL}$ comes from the contribution related to the flat band. As seen from Fig. 3, when the

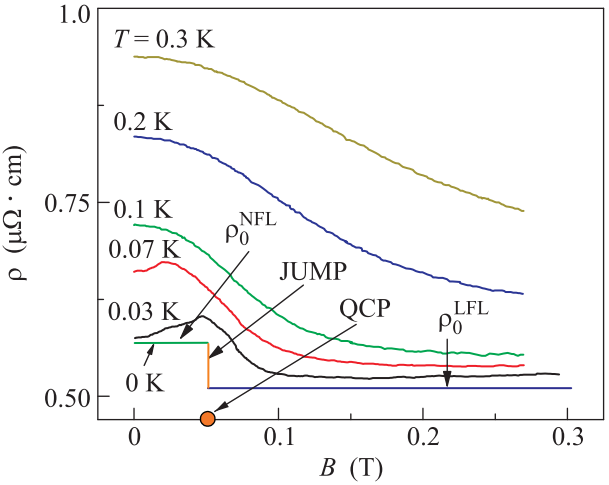

Fig. 3. (Color online) Experimental results [16] for the longitudinal magnetoresistivity $\rho(T,B)$ of $YbRh_2Si_2$ versus B at various temperatures T. The maxima of the curves for $T = 0.03$ and 0.07 K correspond to boundary points of the AF ordered state shown in Fig. 2b. The solid lines marked with 0 K represent the schematic behavior of the residual resistivity ρ_0 as a function of B. The arrows pointing to the horizontal solid lines identify the residual resistivities $\rho_0^{\rm NFL}$ and $\rho_0^{\rm LFL}$ in $YbRh_2Si_2$. The jump of ρ_0 occurs at the QCP identified by an arrow

system transits from the NFL state to the LFL state at fixed T and under application of elevated magnetic fields B, the step-like drop in its resistivity $\rho(T,B)$ becomes more pronounced (see the experimental curves for $T = 0.3, 0.2, 0.1$ K). This behavior is a simple consequence of the fact that the width of the crossover regime is proportional to T. On zooming into the vicinity of

QCP shown in Fig. 3 (corresponding for example to the experimental curves for $T = 0.07$ and 0.03 K), it may be seen that the crossover width remains proportional to temperature, ultimately shrinking to zero and leading to the abrupt jump in the residual resistivity at $T = 0$ when the system crosses the QCP at $B = B_{c0}$. In the same way, application of a magnetic field B to $CeCoIn_5$ causes a step-like drop in its residual resistivity, as is in fact found experimentally [33]. Based on this reasoning, we expect that the higher the quality of both $CeCoIn_5$ and $YbRh_2Si_2$ single crystals, the greater is the ratio $\rho_0^{\rm NFL}/\rho_0^{\rm LFL}$, since the contribution coming from the impurities diminishes and $\rho_0^{\rm NFL}$ approaches ρ_0^c. It is also expected from Eq. (12) that the observed difference ρ_0^c in the residual resistivities will not show a marked dependence on the imperfection of the single crystal unless the impurities destroy the flat band. Finally, we point out that the jump of the magnetoresistivity at zero temperature contradicts the usual behavior of Kondo systems, with the width of the transition remaining finite at $T \to 0$ [17, 20]. Moreover, the Kondo systems has nothing to do with the dissymmetrical tunnelling conductance as a function of the applied voltage V that was predicted to emerge in such HF metals with the flat band as $CeCoIn_5$ and $YbRh_2Si_2$ [7, 34, 35]. Indeed, experimental observations have revealed that the conductance is the dissymmetrical function of V in both $CeCoIn_5$ [36] and $YbRh_2Si_2$ [29].

The emergence of a flat band entails a change of the Hall coefficient $R_{\rm H} = \sigma_{xyz}/\sigma_{xx}^2$ [37, 38]. In homogeneous matter at $B \to 0$ one has $\sigma_{xx} = \sigma/3$, while σ_{xyz} is recast to

$$\sigma_{xyz} = \frac{e^3}{3\gamma^2}\int\left(\frac{dz}{dp}\right)^2\frac{\partial n(z)}{\partial z}dz, \qquad (13)$$

where $n(z)$ is the quasiparticle distribution function. Far from the QCP, these formulas lead to the standard result $R_{\rm H} = 1/Ne$, whereas in the vicinity of the QCP, one finds $R_{\rm H} = K/Ne$ with $K \simeq 1.5$ [38]. We see then that the effective volume of the Fermi sphere shrinks considerably at the QCP. Importantly, in the LFL state where the effective mass stays finite, the value $K = 1$ holds even quite close to the QCP. As we have learned, the width $W(B)$ tends to zero at the QCP, implying that the critical behavior of K at $T \to 0$ emerges abruptly, producing a jump in the Hall coefficient, while the height of the jump remains finite. It is instructive to consider the physics of this jump of $R_{\rm H}$ in the case of $YbRh_2Si_2$. At $T = 0$, the critical magnetic field B_{c0} destroying the AF phase is determined by the condition that the ground-state energy of the AF phase be equal to the ground-state energy of the HF liquid in the LFL paramagnetic state. Hence, at $B \to B_{c0}$ the Néel temperature $T_{\rm N}$ tends to zero. In the measurements of the Hall coefficient $R_{\rm H}$ as a function of B performed in $YbRh_2Si_2$ [17, 18, 39], a jump is detected in $R_{\rm H}$ as $T \to 0$ when the applied magnetic field reaches its critical value $B = B_{c0}$ and then becomes infinitesimally higher at $B = B_{c0} + \delta B$. At $T = 0$, application of the critical magnetic field B_{c0}, which suppresses the AF phase whose Fermi momentum is $p_{\rm F}$, restores the LFL phase with a Fermi momentum $p_f > p_{\rm F}$. This occurs because the quasiparticle distribution function becomes multiply connected and the number of mobile electrons does not change [7]. The AF state can then be viewed as having a "small" Fermi surface characterized by the Fermi momentum $p_{\rm F}$, whereas the LFL paramagnetic ground state at $B > B_{c0}$ has a "large" Fermi surface with $p_f > p_{\rm F}$. As a result, the Hall coefficient experiences a sharp jump because $R_{\rm H}(B) \propto 1/p_F^3$ in the AF phase and $R_H(B) \propto 1/p_f^3$ in the paramagnetic phase. Assuming that $R_{\rm H}(B)$ is a measure of the Fermi momentum [37, 39] (as is the case with a simply connected Fermi volume), we obtain [7, 40]

$$\frac{R_{\rm H}(B = B_{c0} - \delta)}{R_{\rm H}(B = B_{c0} + \delta)} \simeq 1 + 3\frac{p_f - p_{\rm F}}{p_{\rm F}}. \qquad (14)$$

These observations are in excellent agreement with the experimental facts collected on $YbRh_2Si_2$ [17, 18].

Violation of the Wiedemann–Franz law at the QCP in HF metals was predicted and estimated a few years ago [7, 41] and recently observed [19]. Predictions of LFL theory fail in the vicinity of a QCP where the effective mass M^* diverges, since the sp spectrum possesses a flat band at that point. In a once-standard scenario for such a QCP [10, 11], the divergence of the effective mass is attributed to vanishing of the quasiparticle weight Z. However, as already indicated, this scenario is flawed [12]. We therefore employ a different scenario for the QCP, in which the departure of the Lorenz number L from the Wiedemann–Franz value is associated with a rearrangement of sp degrees of freedom leading to a flat band. Within the quasiparticle paradigm, the relation between the Seebeck thermodynamic coefficient S and the conductivities σ and κ has the form [42, 43]

$$\frac{\kappa(T)}{\sigma(T)T} + S^2(T) = \frac{1}{e^2}\frac{I_2(T)}{I_0(T)}. \qquad (15)$$

Here

$$S(T) = \frac{1}{e}\frac{I_1(T)}{I_0(T)}, \qquad (16)$$

with

$$I_k(T) = -\int\left[\frac{\epsilon(p)}{T}\right]^k\left[\frac{d\epsilon(p)}{dp}\right]^2\tau(\epsilon,T)\frac{\partial n(p)}{\partial\epsilon(p)}dv, \qquad (17)$$

where τ is the collision time, dv is the volume element of momentum space, and $n(p)$ is given by Eq. (2) with $\epsilon = \varepsilon - \mu$. Overwhelming contributions to the integrals I_k come from a narrow vicinity $|\epsilon| \sim T$ of the Fermi surface. In case of LFL, the Seebeck coefficient $S(T)$ vanishes linearly with T at $T \to 0$. Then, the group velocity can be factored out from the integrals (17). The same is true for the collision time τ, which at $T \to 0$ depends merely on impurity scattering, and one obtains $I_1(T = 0) = 0$ and $I_2(T \to 0)/I_0(T \to 0) = \pi^2/3$. Inserting these results into Eq. (15), we do find that the Wiedemann–Franz law holds, even if several bands cross the Fermi surface simultaneously [42]. On the other hand, taking into account the fact that the reduction of the ratio L/L_0 occurs in the NFL state at the QCP [41], we conclude that the violation of the Wiedemann–Franz law takes place in the narrow segment of the $T-B$ phase diagram displayed in Fig. 2 having width $W \to 0$ at $T \to 0$. In other words, at $T \to 0$ the ratio L/L_0 becomes abruptly $L/L_0 \sim 0.9$ at $B/B_{c0} = 1$, while $L/L_0 = 1$ at $B/B_{c0} \neq 1$ when the system is in its AF or LFL state shown in Fig. 2. This observation is in a good agreement with experimental facts collected on $YbRh_2Si_2$ [19]. We conclude that at $T \to 0$, the WF law holds in the LFL state at which the Fermi distribution function given by Eq. (2) is reduced to the step function. The violation at $B = B_{c0}$ and at $T \to 0$ seen in $YbRh_2Si_2$ thus suggests that a sharp Fermi surface does exist at $B/B_{c0} \neq 1$ but does not exist only at $B/B_{c0} = 1$ where the flat band emerges.

Among other features, Fig. 4 includes results (solid lines) for the characteristic temperatures $T_{\rm inf}(B)$ and $T_M(B)$, which represent the positions of the kinks separating the energy scales identified experimentally in Refs. [16, 17, 44]. The boundary between the NFL and LFL phases is indicated by a dashed line, while AF labels the antiferromagnetic phase; again the corresponding data are taken from Refs. [16, 17, 44]. It is seen that our calculations are in accord with the experimental facts. In particular, we conclude that the energy scales and the widths W and T^* are reproduced by Eqs. (5) and (7) and related to the special points $T_{\rm inf}$ and T_M associated with the normalized effective mass $M^*_{\rm N}$, which are marked with arrows in the inset and main panel of Fig. 1 [7, 45].

In summary, we have shown that imposition of a magnetic field on $YbRh_2Si_2$ leads to the emergence of the quantum critical point at which a strong suppression of the residual resistivity ρ_0 is accompanied both by a jump of the Hall resistivity and a violation of the Wiedemann–Franz law. The close similarity between the behaviors of the Hall coefficient $R_{\rm H}$, magnetoresistivity ρ, and Lorenz number L at the QCP indicates that all transport measures reflect the same underlying physics, which unambiguously entails an interpretation of the QCP as arising from a fermion condensation quantum phase transition leading to the formation of a flat band.

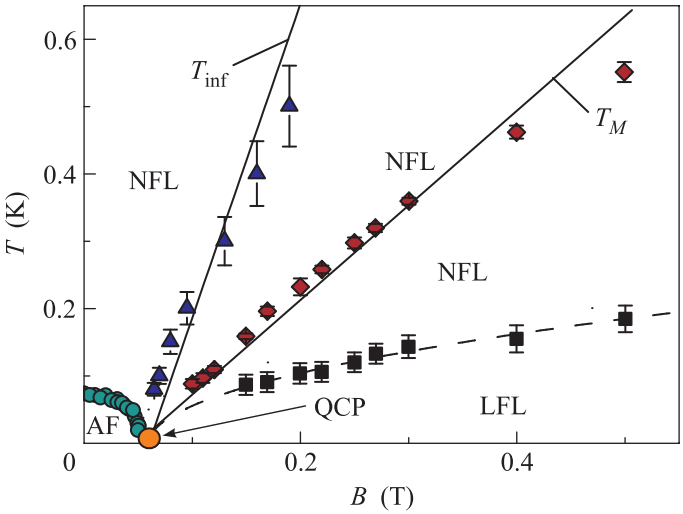

Fig. 4. (Color online) Temperature versus magnetic field $T-B$ phase diagram for $YbRh_2Si_2$. Solid circles represent the boundary between AF and NFL states and the QCP shown by the arrow. Solid squares refer to the boundary between NFL and LFL regimes [16, 17] represented by the dashed line, which is approximated by $(B - B_{c0})^{1/2}$ [7]. Diamonds mark the maxima T_M of the specific heat C/T [44], which are approximated by $T_M \propto b_1(B - B_{c0})$, with b_1 a fitting parameter [7]. Triangles close to the solid line refer to the inflection points $T_{\rm inf}$ in the longitudinal magnetoresistivity [16, 17], while the solid line tracks the function $T_{\rm inf} \propto b_2(B - B_{c0})$, with b_2 a fitting parameter

We thank A. Alexandrov for fruitful discussions. This work was supported by the U.S. DOE, Division of Chemical Sciences, Office of Basic Energy Sciences and the Office of Energy Research, AFOSR, as well as the McDonnell Center for the Space Sciences.

1. G. R. Stewart, Rev. Mod. Phys. **73**, 797 (2001).
2. H. v. Löhneysen, A. Rosch, M. Vojta, and P. Wölfle, Rev. Mod. Phys. **79**, 1015 (2007).
3. P. Gegenwart, Q. Si, and F. Steglich, Nature Phys. **4**, 186 (2008).
4. S. Sachdev, Nature Phys. **4**, 173 (2008).
5. P. Coleman and A. J. Schofield, Nature **433**, 226 (2005).
6. K. Kadowaki and S. B. Woods, Solid State Commun. **58**, 507 (1986).
7. V. R. Shaginyan, M. Ya. Amusia, A. Z. Msezane, and K. G. Popov, Phys. Rep. **492**, 31 (2010).

8. V. R. Shaginyan, Physics of Atomic Nuclei **74**, 1107 (2011).
9. V. A. Khodel, J. W. Clark, and M. V. Zverev, Physics of Atomic Nuclei **74**, 1230 (2011).
10. P. Coleman, C. Pepin, Q. Si, and R. Ramazashvili, J. Phys. Condens. Matter **13**, R723 (2001).
11. P. Coleman and C. Pepin, Physica B **312–313**, 383 (2002).
12. V. A. Khodel, JETP Lett. **86**, 721 (2007).
13. J. W. Clark, V. A. Khodel, and M. V. Zverev, Int. J. Mod. Phys. B **24**, 4901 (2010).
14. V. A. Khodel and V. R. Shaginyan, JETP Lett. **51**, 553 (1990).
15. G. E. Volovik, Lect. Notes in Physics **718**, 31 (2007).
16. P. Gegenwart et al., Science **315**, 969 (2007).
17. S. Friedemann et al., Proc. Natl. Acad. Sci. USA **107**, 14547 (2010).
18. S. Friedemann et al., J. Phys.: Condens. Matter **23**, 094216 (2011).
19. H. Pfau et al., Nature **484**, 493 (2012).
20. P. Schlottmann, Z. Phys. B: Condens Matter **51**, 223 (1983).
21. D. Pines and P. Noziéres, *Theory of Quantum Liquids*, Benjamin, N.Y., 1966.
22. P. Nozières, J. Phys. I France **2**, 443 (1992).
23. J. W. Clark, V. A. Khodel, and M.V. Zverev, Phys. Rev. B **71**, 012401 (2005).
24. P. Gegenwart et al., Phys. Rev. Lett. **89**, 056402 (2002).
25. V. R. Shaginyan, JETP Lett. **79**, 286 (2004).
26. D. Takahashi et al., Phys. Rev. B **67**, 180407 (2003).
27. J. Custers et al., Nature **424**, 524 (2003).
28. V. A. Khodel and M. V. Zverev, JETP Lett. **85**, 404 (2007).
29. S. Ernst et al., Nature **474**, 363 (2011).
30. V. R. Shaginyan, A. Z. Msezane, K. G. Popov et al., Phys. Rev. B **86**, 085147 (2012).
31. P. Aynajian et al., Nature **486**, 201 (2012).
32. S. Hikami, A. I. Larkin, and Y. Nagaoka, Prog. Theor. Phys. **63**, 707 (1980).
33. J. Paglione et al., Pys. Rev. Lett. **91**, 246405 (2003).
34. V. R. Shaginyan, JETP Lett. **81**, 222 (2005).
35. V. R. Shaginyan and K. G. Popov, Phys. Lett. A **361**, 406 (2007).
36. W. K. Park and L. H. Greene, J. Phys.: Condens. Matter **21**, 103203 (2009).
37. M. R. Norman, Q. Si, Ya. B. Bazaliy, and R. Ramazashvili, Phys. Rev. Lett. **90**, 116601 (2002).
38. V. A. Khodel, M. V. Zverev, and J. W. Clark, JETP Lett. **81**, 315 (2005).
39. S. Paschen et al., Nature **432**, 881 (2004).
40. V. R. Shaginyan, P. G. Popov, and S. A. Artamonov, JETP Lett. **82**, 215 (2005).
41. V. A. Khodel, V. M. Yakovenko, and M. V. Zverev, JETP Lett. **86**, 772 (2007).
42. E. M. Lifshitz and L. P. Pitaevskii, *Physical Kinetics*, Pergamon Press, Oxford, 1981.
43. N. W. Ashkroft and N. D. Mermin, *Solid State Physics*, HRW, Philadelphia, 1976.
44. N. Oeschler et al., Physica B **403**, 1254 (2008).
45. V. R. Shaginyan et al., Phys. Lett. A **373**, 986 (2009).